Engineering the Multifunctionality of $Li_3Y_3Te_2O_{12}$ Garnet with Sm^{3+} and Tb^{3+} Activators for Solid-State Lighting and Luminescence Thermometry

*Amrithakrishnan Bindhu, Jawahar I. Naseemabeevi, Subodh Ganesanpotti**

Department of Physics, University of Kerala, Kariavattom Campus, Thiruvananthapuram, Kerala - 695 581, India

E-mail: gsubodh@gmail.com, gsubodh@keralauniversity.ac.in

Supplementary data

Table S1. The percentage difference of ionic radii (D_r) between host cations and Sm^{3+} ions.

Host cation (CN)	Activator ion (CN)	R_m (Å)	R_d (Å)	D_r (%)
Li^+ (4)	Sm^{3+} (8)	0.59(4)	1.027	-82.8
Y^{3+} (8)	Sm^{3+} (8)	1.01(9)	1.027	-5.9
Te^{6+} (6)	Sm^{3+} (8)	0.56(6)	1.027	-92.7

Table S2. Comparison of $T_{1/2}$ of reported Sm^{3+} based phosphors.

Compositions	$T_{1/2}$ (K)	References
$Li_3Ba_2La_3(MoO_4)_8$: Sm^{3+}	512	[1]
$Li_6CaLa_{1.94}Sm_{0.06}Ta_2O_{12}$	423	[2]
Ca_2MgTeO_6:Sm^{3+}	>480	[3]
$Li_3Gd_3Te_2O_{12}$:Sm^{3+}	>480	[4]
$Ca_2Al_2SiO_7$:Sm^{3+}	>500	[5]
$Sr_9In(PO_4)_7$: Sm^{3+}	>523	[6]
$NaSrLa(MoO_4)O_3$: Sm^{3+}	423	[7]
$Li_3Y_3Te_2O_{12}$: Sm^{3+}	500	This work

Table S3. Rietveld refinement and crystallographic data of $Li_3Y_3Te_2O_{12}$: 0.05 Tb^{3+}, 0.07 Sm^{3+} phosphor.

Formula	$Li_3Y_{2.88}Tb_{0.05}Sm_{0.07}Te_2O_{12}$
Crystal system	Cubic
Space group	$Ia\overline{3}d$ (230, O_h^{10})
Cell Parameters	a= 12.2596(1) Å
Reliability factors	R_{wp}= 3.40 %, R_p= 2.63 % and GOF= 1.56

Atom	Site	X	y	Z	Occupancy	B_{iso} (Å^2)
$Y^{3+}/Tb^{3+}/Sm^{3+}$	24c	0.125	0.00	0.25	1	0.007(9)
Te^{6+}	16a	0.00	0.00	0.00	1	0.006(9)
Li^{3+}	24d	0.25	0.875	0.00	1	0.018(3)
O^{2-}	96h	0.268(1)	0.110(2)	0.196(8)	1	0.01(1)

Table S4. Comparison of temperature sensing properties of different phosphors.

Phosphors	Temperature range (K)	S_r (% K^{-1})	References
$Ca_2TbSn_2Al_3O_{12}$:Sm^{3+}	300-500	0.50	[8]
$SrY_2(MoO_4)_4$: Tb^{3+}/Sm^{3+}	290-440	0.9	[9]
Ca_2LaTaO_6:Mn^{2+}/Tb^{3+}	300-450	3.6	[10]
$CaGdAlO_4$:Mn^{4+}, Tb^{3+}	200-600	2.23	[11]
$Y_3Al_5O_{12}$:Dy^{3+}/Cr^{3+}	293- 573	2.32	[12]
$Na_3Sc_2P_3O_{12}$: Eu^{2+}/ Mn^{2+}	293-473	1.556	[13]
Sr_2LuTaO_6: Tb^{3+}/Mn^{4+}	313–573	1.98	[14]
$Ba_3(VO_4)_2$: Sm^{3+}	303-463	2.24	[15]
$BaGd_2O_4$: Bi^{3+}/Sm^{3+}	293-473	1.11	[16]
$LaNbO_4$: Bi^{3+}/Eu^{3+}	303-483	1.89	[17]
$Ca_2NaMg_2V_3O_{12}$: Sm^{3+}	303-503	1.889	[18]
$Sr_2NaMg_2V_3O_{12}$: Sm^{3+}	300-500	2.01	[19]
$LaNbO_4$: Bi^{3+}/Tb^{3+}	303-483	2.36	[17]
$Li_3Y_3Te_2O_{12}$: Dy^{3+}	80-300	1.2	[20]
$Li_3Y_3Te_2O_{12}$: Bi^{3+}/Pr^{3+}	300-500	1.8	[21]
$Li_3Y_3Te_2O_{12}$: Sm^{3+}	300-500	1.0	This work
$Li_3Y_3Te_2O_{12}$: Sm^{3+}/Tb^{3+}	300-500	1.8	This work

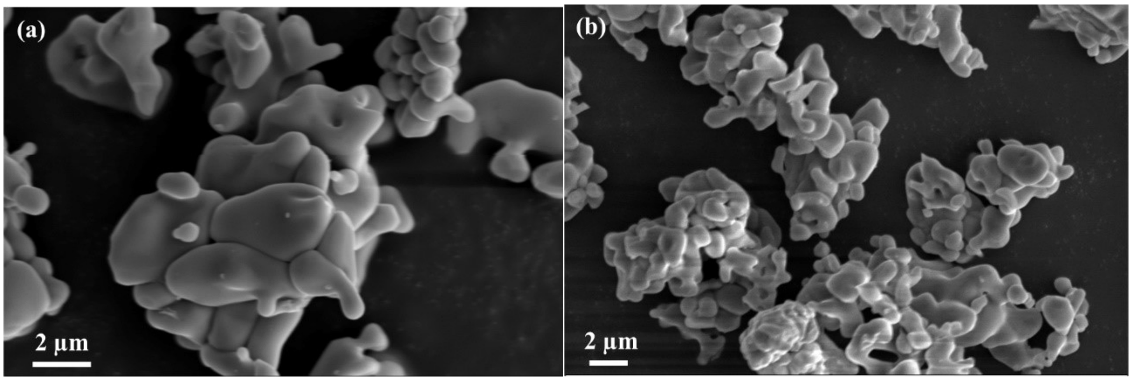
(a)
2 μm
(b)
2 μm

Fig. S1 SEM images of (a) LYTO, and (b) LYTO: 0.05 Sm^{3+} phosphors.

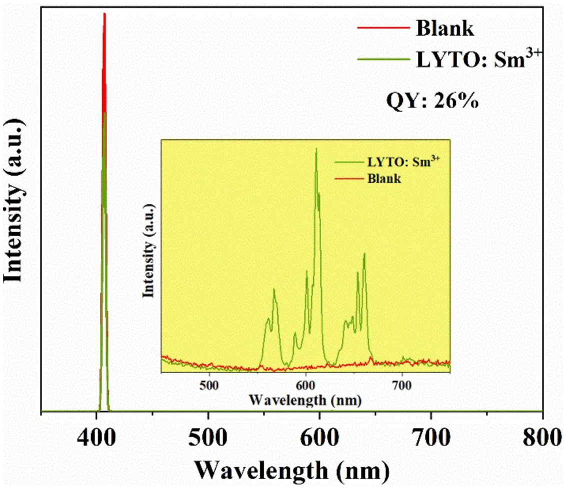

Fig. S2 Quantum yield of LYTO: Sm^{3+} under 407 nm excitation and 611 nm emission wavelength.

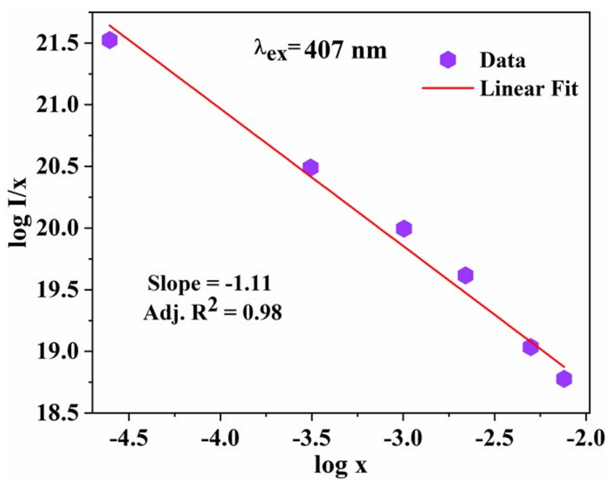

Fig. S3 The log(I/x)-log(x) plot for the transition of Sm^{3+} ions in LYTO: Sm^{3+} phosphor.

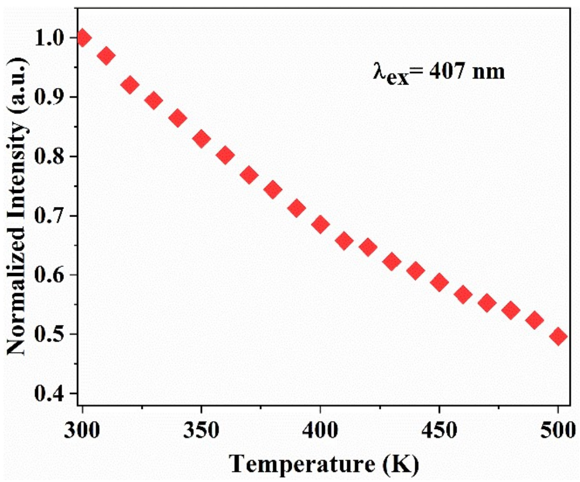

Fig. S4 The variation of emission intensity of LYTO: Sm^{3+} with temperature.

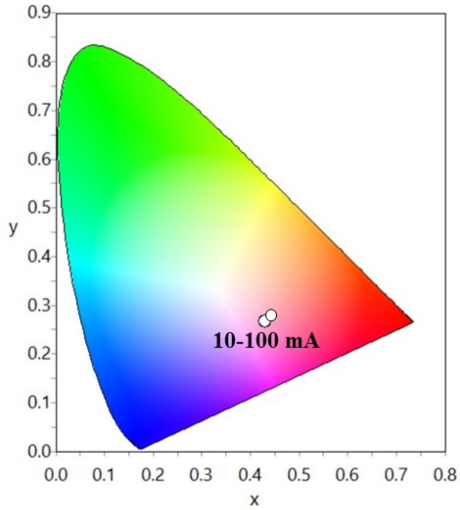

Fig. S5 The shift of CIE coordinates of the fabricated LED at higher input bias currents.

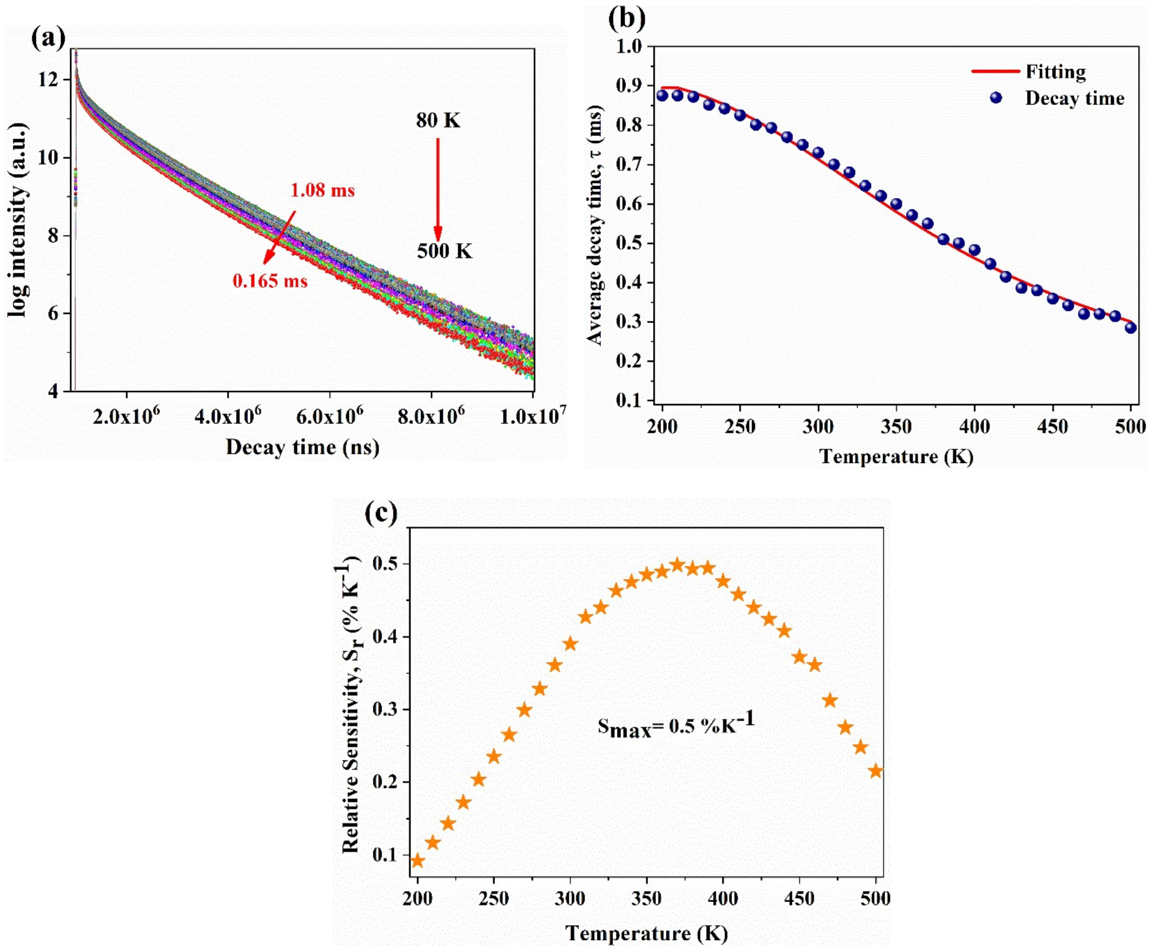

Fig. S6 (a) The temperature-dependent decay curves of LYTO: Sm phosphor, (b) the average decay time with temperature, and (c) the dependence of relative sensitivity, Sr Vs. T in LYTO: Sm phosphor determined by decay time method.

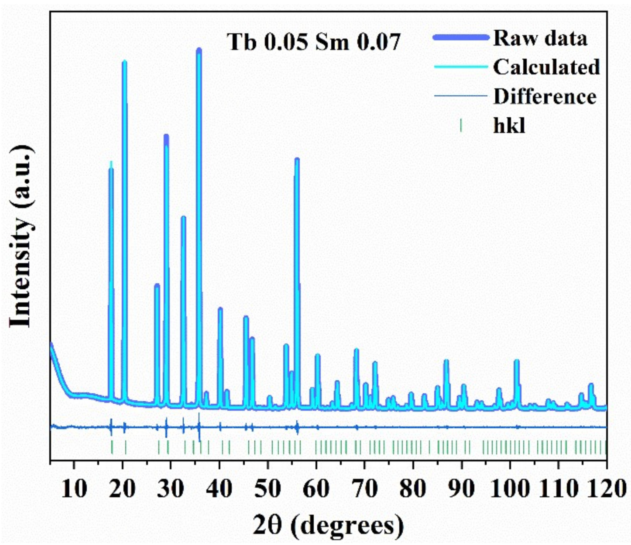

Fig. S7 The Rietveld refinement pattern of $Li_3Y_3Te_2O_{12}$: 0.05 Tb^{3+}, 0.07 Sm^{3+} phosphor.

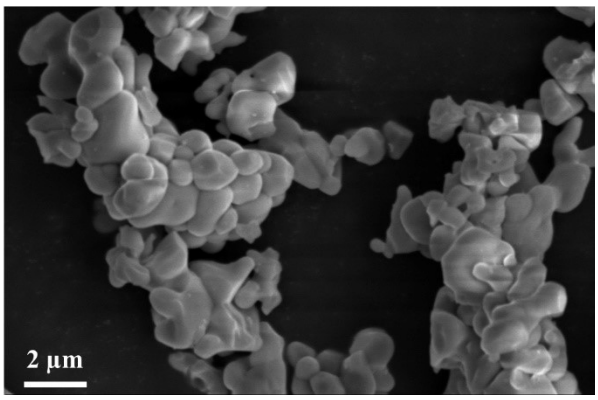

Fig. S8 SEM images of LYTO: Sm^{3+}, Tb^{3+} phosphors.

References

[1] F. Baur, A. Katelnikovas, S. Sakirzanovas, R. Petry, T. Jüstel, Synthesis and Optical Properties of $Li_3Ba_2La_3(MoO_4)_8$: Sm^{3+} Powders for pcLEDs, Zeitschrift Für Naturforschung B 69 (2014) 183–192. https://doi.org/10.5560/znb.2014-3279.

[2] Y. V. Baklanova, L.G. Maksimova, O.A. Lipina, A.P. Tyutyunnik, V.G. Zubkov, Novel orange-red-emitting $Li_{5+x}Ca_xLa_{3-x}Ta_2O_{12}$:$Sm^{3+}$ (x = 0; 1) phosphors: Crystal structure, luminescence and thermal quenching studies, J Lumin 224 (2020) 117315. https://doi.org/10.1016/J.JLUMIN.2020.117315.

[3] L. Zhang, J. Che, Y. Ma, J. Wang, R. Kang, B. Deng, R. Yu, H. Geng, Luminescent and thermal properties of novel orange-red emitting Ca_2MgTeO_6:Sm^{3+} phosphors for white LEDs, J Lumin 225 (2020) 117374. https://doi.org/10.1016/j.jlumin.2020.117374.

[4] Z. Gao, N. Xue, J.H. Jeong, R. Yu, Spectroscopic properties of a novel garnet-type tellurate orange-red emitting $Li_3Gd_3Te_2O_{12}$:Sm^{3+} phosphor, Journal of Materials Science: Materials in Electronics 28 (2017) 12640–12645. https://doi.org/10.1007/S10854-017-7088-Y/FIGURES/10.

[5] N.M. Son, D.T. Tien, N.T.Q. Lien, V.X. Quang, N.N. Trac, T.T. Hong, H. Van Tuyen, Luminescence and Thermal-Quenching Properties of Red-Emitting $Ca_2Al_2SiO_7$:Sm^{3+} Phosphors, J Electron Mater 49 (2020) 3701–3707. https://doi.org/10.1007/S11664-020-08086-X/METRICS.

[6] K. Su, Q. Zhang, X. Yang, B. Ma, Crystal structure and luminescence properties of thermally stable Sm^{3+}-doped $Sr_9In(PO_4)_7$ orange-red phosphor, J Phys D Appl Phys 53 (2020) 385101. https://doi.org/10.1088/1361-6463/AB938D.

[7] J. Xue, M. Song, H.M. Noh, S.H. Park, B.R. Lee, J.H. Kim, J.H. Jeong, Near-ultraviolet light induced red emission in Sm^{3+}-activated $NaSrLa(MoO_4)O_3$ phosphors for solid-state illumination, J Alloys Compd 817 (2020) 152705. https://doi.org/10.1016/J.JALLCOM.2019.152705.

[8] Z. Zhang, J. Yan, Q. Zhang, G. Tian, W. Jiang, J. Huo, H. Ni, L. Li, J. Li, Enlarging Sensitivity of Fluorescence Intensity Ratio-Type Thermometers by the Interruption of the Energy Transfer from a Sensitizer to an Activator, Inorg Chem 61 (2022) 16484–16492. https://doi.org/10.1021/acs.inorgchem.2c02756.

[9] I. Kachou, M. Dammak, S. Auguste, F. Amiard, P. Daniel, A novel optical temperature sensor and energy transfer properties based on Tb $^{3+}$ /Sm $^{3+}$ codoped $SrY_2(MoO_4)_4$ phosphors, Dalton Transactions 52 (2023) 18233–18246. https://doi.org/10.1039/D3DT03410K.

[10] Y. Chen, G. Li, Y. Ding, Q. Mao, M. Liu, C. Wang, R. Zheng, B.-L. Su, J. Zhong, Antithermal Quenching and Multiparametric Temperature Sensing from Mn^{2+}/Tb^{3+} -Codoped Ca_2LaTaO_6 Phosphor, Adv Photonics Res 4 (2023). https://doi.org/10.1002/adpr.202300106.

[11] Y. Fang, Y. Zhang, Y. Zhang, J. Hu, Achieving high thermal sensitivity from ratiometric $CaGdAlO_4$: Mn^{4+},Tb $^{3+}$ thermometers, Dalton Transactions 50 (2021) 13447–13458. https://doi.org/10.1039/D1DT02185K.

[12] D. Chen, S. Liu, Y. Zhou, Z. Wan, P. Huang, Z. Ji, Dual-activator luminescence of RE/TM:$Y_3Al_5O_{12}$ (RE = Eu^{3+}, Tb^{3+}, Dy^{3+}; TM = Mn^{4+}, Cr^{3+}) phosphors for self-referencing optical thermometry, J Mater Chem C Mater 4 (2016) 9044–9051. https://doi.org/10.1039/c6tc02934e.

[13] X. Zhang, Z. Zhu, Z. Guo, Z. Sun, Y. Chen, A ratiometric optical thermometer with high sensitivity and superior signal discriminability based on $Na_3Sc_2P_3O_{12}$: Eu^{2+}, Mn^{2+} thermochromic phosphor, Chemical Engineering Journal 356 (2019) 413–422. https://doi.org/10.1016/J.CEJ.2018.09.075.

[14] Y. Zhang, B. Sun, J. Liu, Z. Zhang, H. Liu, Luminescence and energy transfer performances of Tb^{3+}/Mn^{4+} co-doped Sr_2LuTaO_6 double-perovskite phosphors for a highly sensitive optical thermometer, Dalton Transactions 52 (2023) 13304–13315. https://doi.org/10.1039/D3DT02270F.

[15] P. Du, Y. Hua, J.S. Yu, Energy transfer from VO_4^{3-} group to Sm^{3+} ions in $Ba_3(VO_4)_2$:3xSm^{3+} microparticles: A bifunctional platform for simultaneous optical thermometer and safety sign, Chemical Engineering Journal 352 (2018) 352–359. https://doi.org/10.1016/J.CEJ.2018.07.019.

[16] J. Fu, L. Zhou, Y. Chen, J. Lin, R. Ye, D. Deng, L. Chen, S. Xu, Dual-mode optical thermometry based on Bi^{3+}/Sm^{3+} co-activated BaGd2O4 phosphor with tunable sensitivity, J Alloys Compd 897 (2022) 163034. https://doi.org/10.1016/J.JALLCOM.2021.163034.

[17] J. Xue, Z. Yu, H.M. Noh, B.R. Lee, B.C. Choi, S.H. Park, J.H. Jeong, P. Du, M. Song, Designing multi-mode optical thermometers via the thermochromic $LaNbO_4$:Bi^{3+}/Ln^{3+} (Ln = Eu, Tb, Dy, Sm) phosphors, Chemical Engineering Journal 415 (2021) 128977. https://doi.org/10.1016/J.CEJ.2021.128977.

[18] H. Zhou, N. Guo, X. Lü, Y. Ding, L. Wang, R. Ouyang, B. Shao, Ratiometric and colorimetric fluorescence temperature sensing properties of trivalent europium or

samarium doped self-activated vanadate dual emitting phosphors, J Lumin 217 (2020) 116758. https://doi.org/10.1016/J.JLUMIN.2019.116758.

[19] A. Bindhu, J.I. Naseemabeevi, S. Ganesanpotti, Delving into the multifunctionality of $Sr_2NaMg_2V_3O_{12}$via RE^{3+} substitution for dual-mode temperature sensing, latent fingerprint detection and security inks, Mater Adv 4 (2023) 3796–3812. https://doi.org/10.1039/D3MA00241A.

[20] A. Bindhu, J.I. Naseemabeevi, S. Ganesanpotti, Insights into the crystal structure and photophysical response of Dy^{3+} doped $Li_3Y_3Te_2O_{12}$ for ratiometric temperature sensing, Journal of Science: Advanced Materials and Devices 7 (2022) 100444. https://doi.org/10.1016/J.JSAMD.2022.100444.

[21] A. Bindhu, A.S. Priya, J.I. Naseemabeevi, S. Ganesanpotti, Deciphering crystal structure and photophysical response of Bi^{3+} and Pr^{3+} co-doped $Li_3Gd_3Te_2O_{12}$ for lighting and ratiometric temperature sensing, J Alloys Compd 893 (2022). https://doi.org/10.1016/j.jallcom.2021.162246.